THE JOURNAL OF PHYSICAL CHEMISTRY B

Article

pubs.acs.org/JPCB

n-Butanol Partitioning and Phase Behavior in DPPC/DOPC Membranes

Yogi Kurniawan,[†] Keerthi P. Venkataramanan,[‡] Carmen Scholz,[§] and Geoffrey D. Bothun*[,†]

[†]Department of Chemical Engineering, University of Rhode Island, 16 Greenhouse Rd, Kingston, Rhode Island 02881, United States

[‡]Biotechnology Science and Engineering program, University of Alabama in Huntsville, 301 Sparkman Dr., Huntsville, Alabama 35899, United States

[§]Department of Chemistry, University of Alabama in Huntsville, 301 Sparkman Dr., Huntsville, Alabama 35899, United States

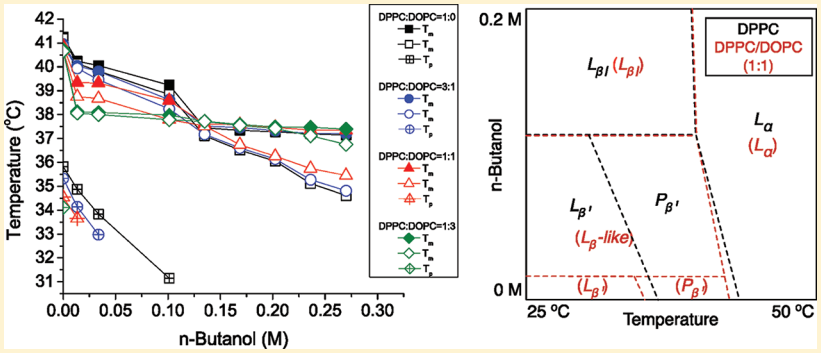

ABSTRACT: Membrane phase behavior and fluidization have been examined in heterogeneous membranes composed of dipalmitoylphosphatidylcholine (DPPC, a saturated lipid) and dioleoylphosphatidylcholine (DOPC, an unsaturated lipid) at *n*-butanol concentrations below and above the interdigitation threshold of DPPC. Our results show that the presence of DOPC did not influence the interdigitation concentration of *n*-butanol on DPPC (0.1−0.13 M) despite the fact that DOPC increased *n*-butanol partitioning into the membranes. When DPPC was the continuous phase, up to equimolar DPPC:DOPC, *n*-butanol partitioning into gel or interdigitated DPPC was only slightly affected by the presence of DOPC. In this case a "cooperative effect" of DOPC + *n*-butanol eliminated the DPPC pretransition phase and yielded an untilted gel-like phase. When DOPC was the continuous phase, more *n*-butanol was needed to cause DPPC interdigitation (0.2 M), which was attributed to *n*-butanol residing at the interface between DOPC and DPPC domains. To our knowledge, this is the first study to examine the effects of *n*-butanol partitioning on membranes composed of saturated and unsaturated lipids that exhibit coexisting phase states.

INTRODUCTION

The partitioning of primary alcohols into homogeneous lipid bilayer membranes has been well studied. Generally speaking, the partitioning of short alcohols (up to C_6) dehydrates lipid headgroups at the membrane/water interface, reduces membrane surface tension, leads to a reduction in lipid ordering (i.e., membrane fluidization), and, at high concentrations, causes lipid interdigitation.[1−12] As the carbon-chain length of the alcohol increases, the partitioning coefficient increases and fluidization or interdigitation occurs at lower alcohol concentrations. While well characterized in homogeneous membranes, there has been relatively little work on alcohol partitioning and its effects on heterogeneous membranes that contain multiple lipid species and coexisting phase states.

This work examines *n*-butanol partitioning and membrane restructuring which, compared to ethanol, have not been examined extensively. *n*-Butanol is a viable biofuel and platform chemical for biorefining. It is also lipophilic and, when produced by fermentation, partitions into microbial membranes and compromises membrane integrity.[13,14] This can ultimately inhibit or eliminate microbial activity. Microorganisms respond by altering their lipid composition, specifically the ratio of saturated to unsaturated lipids and/or lipid tail length, to maintain a homeoviscous membrane state.[14] Studying the effects of *n*-butanol on heterogeneous membranes composed of saturated and unsaturated lipids is an important step toward understanding this response mechanism.

One common way to probe the effects of an alcohol on the membrane structure is through lipid phase behavior (Figure 1). In homogeneous membranes composed of saturated lipids, such as dipalmitoylphosphatidylcholine (DPPC), *n*-butanol partitioning can disorder the lipids and reduce the pretransition and melting temperatures.[8,12] Above a threshold concentration (0.14−0.18 M)[4,12] *n*-butanol leads to complete lipid interdigitation. Previous work has shown that short-chain alcohols exhibit greater partitioning into unsaturated lipid membranes than into saturated membranes. Alcohols partition into the lipid/water interface, and greater partitioning into

Received: February 9, 2012
Revised: April 30, 2012
Published: April 30, 2012

   dx.doi.org/10.1021/jp301340k | *J. Phys. Chem. B* 2012, 116, 5919−5924

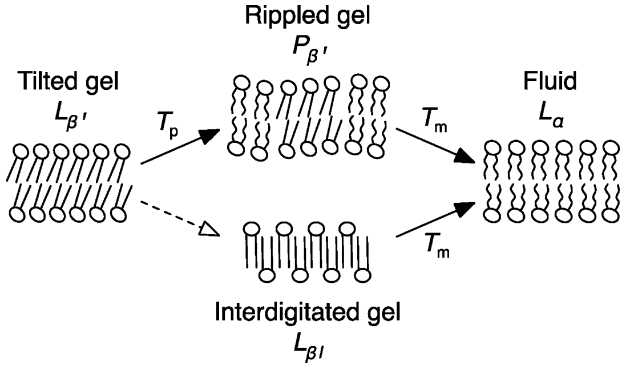

Figure 1. Schematic of membrane phase behavior and nomenclature. With heating, a tilted gel to rippled gel transition, $L_{\beta'} \rightarrow P_{\beta'}$, occurs at the pretransition temperature (T_p), and a rippled gel to fluid transition, $P_{\beta'} \rightarrow L_\alpha$, occurs at the main transition or melting temperature (T_m). At a critical alcohol concentration the titled gel phase becomes interdigitated, $L_{\beta'} \rightarrow L_{\beta I}$, and the pretransition is eliminated.

unsaturated lipid membranes can be attributed to a greater interfacial area stemming from the packing properties of unsaturated acyl tails.[10,15] It is unclear what effect this might have on the phase behavior of a heterogeneous membrane with saturated and unsaturated lipids. Using atomic force microscopy, Marques et al.[16] have shown that phase separation in DPPC/dioleoylphosphatidylcholine (DOPC) membranes caused by ethanol is dependent on which lipid phase is continuous. When DOPC was continuous at low ethanol concentrations, ethanol preferentially partitioned into and thinned the fluid DOPC phase. Increasing ethanol concentration then thinned both the DOPC and gel DPPC domains. When gel DPPC was the continuous phase and fluid DOPC domains were present, ethanol first partitioned at the gel/fluid interface and did not lead to the expansion of the fluid domains. These experiments were performed below the ethanol interdigitation concentration.

To our knowledge, the effects of *n*-butanol on heterogeneous membranes have not yet been examined. In this study, DPPC/DOPC liposomes were used as a model system to investigate *n*-butanol partitioning, membrane phase behavior, and membrane fluidization at *n*-butanol concentration up to 0.27 M (20 g/L). The DPPC:DOPC molar ratio was varied to study membranes where DPPC (1:0, 3:1, and 1:1) or DOPC (1:3 and 0:1) was the continuous phase.

EXPERIMENTAL SECTION

1,2-Dipalmitoyl-*sn*-glycero-3-phosphocholine (DPPC, >99% purity) and 1,2-dioleoyl-*sn*-glycero-3-phosphocholine (DOPC, >99% purity) were purchased from Avanti Polar Lipids (Alabaster, AL) and used without further purification. The fluorescent membrane probe, 1,6-diphenyl-1,3,5-hexatriene (DPH, >98%), was purchased from Sigma-Aldrich (St. Louis, MO). HPLC grade *n*-butanol and chloroform were purchased from Fisher Scientific. Deionized (DI) ultrafiltered water was obtained from a Millipore Direct Q-3 purifier.

Liposome Preparation. Liposomes were prepared by the Bangham method.[17] Briefly, DPPC and DOPC dissolved in chloroform were mixed to achieve the desired ratio of DPPC to DOPC. The chloroform was then evaporated under a stream of nitrogen, and the samples were dried under vacuum for at least 30 min. The dry films were then hydrated with 1.5 mL of deionized water to yield a total lipid concentration of 0.5 mM. Liposome suspensions were formed by sonication at 50 °C for 30 min using a bath ultrasonicator (Branson, Danbury, CT). The average liposome diameters are summarized in Table 1.

Table 1. Liposome Hydrodynamic Diameter (d_h) and Polydispersity Index (PDI) Based on Dynamic Light Scattering (DLS)

DPPC:DOPC (molar ratio)	d_h (nm)	PDI
1:0	343	0.282
3:1	271	0.310
1:1	118	0.329
1:3	108	0.366

Butanol was then added to the samples at the desired concentration. The samples were briefly vortexed and stored for 2 h after the butanol addition before further processing or analysis.

High Performance Liquid Chromatography (HPLC). HPLC was one of the two methods to determine the lipid/water *n*-butanol partitioning coefficient. Sample preparation began by taking liposomes (no *n*-butanol) and liposomes + *n*-butanol and centrifuging the suspensions at 10 000 rpm for 30 min at 4 °C (Megafuge 16 R, Germany). The aqueous supernatant was separated from the liposomes and analyzed by HPLC for *n*-butanol concentration. HPLC was conducted with a resin-based column (Aminex HPX-87H, Bio-Rad, CA) and a refractive index detector (Varian, CA) using with 0.5 mM H_2SO_4 as the mobile phase. Standard calibration curves were prepared with aqueous butanol solutions containing 0.007–0.135 M *n*-butanol (R^2 = 0.994).

The partition coefficient, K_p, was calculated as

$$K_p = \frac{x_b^m}{x_b^w} \tag{1}$$

where x_b^m and x_b^w are the mole fractions of *n*-butanol (b) in the membrane (m) and aqueous (w) phases. *n*-Butanol mole fractions were determined based on mole balance, $x_b^m = n_b^m/(n_b^w + n_b^m)$ and $x_b^w = n_b^w/(n_b^w + n_b^m)$, where n_b^m and n_b^w are the number of moles of *n*-butanol in the membrane and aqueous phases, respectively. The number of moles of *n*-butanol in the membrane was calculated as $n_b^m = n_b - n_b^w$, where n_b was the total number of moles of *n*-butanol in the system.

Differential Scanning Calorimetry (DSC). DSC was performed using a TA Instruments Nano DSC with capillary cells. The reference cell was filled with degassed water and the sample cell was filled with 760 μL of degassed sample. The cell chamber was sealed and pressurized to 3 atm under nitrogen. Samples were analyzed by consecutive heating/cooling cycles between 25 and 50 °C at a rate of 1 °C/min. Pretransition temperature, T_p, melting temperature, T_m, and melting enthalpy, ΔH_m, were determined using the Universal Analysis software. The melting temperature was taken as the temperature at maximum peak height.

K_p was calculated from DSC results as

$$\Delta T_m = -\frac{RT_{m,0}^2}{\Delta H_m}\left(\frac{C_b K_p}{C_w + C_l}\right) \tag{2}$$

where ΔT_m is the measured change in melting temperature ($T_m - T_{m,0}$), R is the gas constant, $T_{m,0}$ is the melting temperature of DPPC without *n*-butanol, and ΔH_m is the lipid melting

dx.doi.org/10.1021/jp301340k | J. Phys. Chem. B 2012, 116, 5919–5924

enthalpy. C_b, C_w, and C_l are the *n*-butanol, water, and lipid molar concentrations, respectively.

Fluorescence Anisotropy. Liposome preparation for fluorescence anisotropy was similar to that for DSC. In this case, DPH was added to the lipids in chloroform as a probe at a DPH:lipid molar ratio of 1:400. The samples were hydrated with 3 mL of DI water to yield a total lipid concentration of 0.04 mM. DPH anisotropy, $\langle r \rangle$, in DPPC/DOPC bilayers was measured as a function of *n*-butanol concentration using a LS55 luminescence spectrometer with a Peltier system (Perkin-Elmer, Shelton, CT). Heating and cooling scans were conducted between 25 and 50 °C at a rate of 1 °C/min, and the sample was continuously mixed with a magnetic stirrer. Steady-state DPH anisotropy was determined at an excitation wavelength of 350 nm and an emission wavelength of 452 nm with a 10 nm slit width. The anisotropy was calculated as

$$\langle r \rangle = \frac{I_{VV} - I_{VH}}{I_{VV} + GI_{VH}} \quad (3)$$

where I represents the fluorescence intensity, the subscripts V and H represent the vertical and horizontal orientation of the excitation and emission polarizers, respectively, and G is the grating factor ($G = I_{HV}/I_{VH}$), which accounts for the correction factor of the sensitivity of the instrument toward vertically and horizontally polarized light. Anisotropy is dependent upon the fluorescence lifetime of DPH (τ), which changes with temperature and lipid composition.[18,19] However, in this work steady-state anisotropy was measured, and changes in τ are not considered.

RESULTS

Membrane Phase Behavior. Results are first presented for DPPC with *n*-butanol, which has been previously studied.[4,8,12] DSC was conducted by adding *n*-butanol at room temperature followed by sequential heating and cooling scans (Figure 2). Without *n*-butanol, DPPC underwent a pretransition at 35.8 °C with heating ($L_{\beta'} \rightarrow P_{\beta'}$) and melted at 41.2 °C with heating ($P_{\beta'} \rightarrow L_\alpha$) and 41.1 °C with cooling ($L_\alpha \rightarrow P_{\beta'}$); no pretransition was observed with cooling. Adding *n*-butanol up to 0.1 M decreased T_p to 31.1 °C, and beyond 0.1 M the pretransition disappeared. With respect to T_m, increasing the *n*-butanol concentration up to 0.13 M led to a significant decrease in T_m with no appreciable melting hysteresis between heating and cooling. Above 0.13 M *n*-butanol, T_m plateaued with heating and there was a significant melting hysteresis.

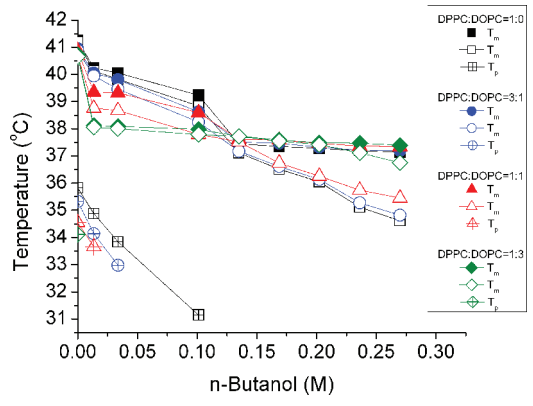

Figure 2. DSC thermographs of membrane phase behavior at DPPC:DOPC ratios of (■, □) 1:0, (blue ●, ○) 3:1, (red ▲, △) 1:1, and (green ◆, ◇) 1:3 as a function of *n*-butanol concentration. Melting temperatures (T_m) are shown as filled symbols for heating and unfilled symbols for cooling scans. Pretransition temperatures (T_p) are shown for heating scans at DPPC:DOPC ratios of (⊞) 1:0, (blue ⊕) 3:1, (red crossed △) 1:1, and (green crossed ◇) 1:3.

Melting enthalpies, ΔH_m, are shown in Figure 3. ΔH_m describes tail disordering and bilayer expansion, which is resisted by interlipid van der Waals attraction.[1,20] Increases in ΔH_m were observed within increasing *n*-butanol concentration, and upon cooling, ΔH_m hysteresis was evident. ΔH_m hysteresis became most pronounced above 0.13 M *n*-butanol. Evidence of lipid interdigitation with increasing *n*-butanol concentration includes the disappearance T_p, a plateauing or increase in T_m, T_m hysteresis, and increases in ΔH_m.[4,12] Interdigitated phases ($L_{\beta I}$) exhibit greater ordering than rippled gel phases ($P_{\beta'}$) and yield higher ΔH_m upon melting. Our results show that DPPC was interdigitated above 0.13 M *n*-butanol ($L_{\beta'} \rightarrow L_{\beta I}$), which is in agreement with previous work.[4,12]

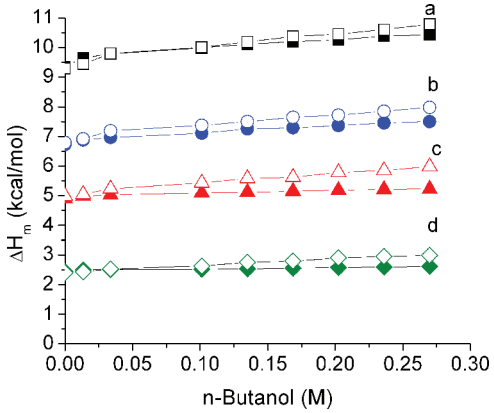

Figure 3. Melting enthalpy as a function of *n*-butanol concentration at different DPPC:DOPC ratios of (a; ■, □) 1:0, (b; blue ●, ○) 3:1, (c; red ▲, △) 1:1, and (d; green ◆, ◇)1:3. Filled symbols represent heating scans and unfilled symbols represent cooling scans.

DOPC had little effect on the T_p or T_m of DPPC in the absence of *n*-butanol, as shown in Figure 2, and confirms the two-phase coexistence of DOPC-rich L_α and DPPC-rich $L_{\beta'}$ phases below the pretransition. At DPPC:DOPC ratios of 3:1 and 1:1, the pretransition disappeared above 0.03 and 0.01 M *n*-butanol, respectively. This indicates that less *n*-butanol was needed to suppress the pretransition with increasing DOPC concentration. With respect to melting, the trends in T_m with increasing *n*-butanol concentration were similar to that for DPPC and suggest that the DPPC/DOPC membranes were interdigitated above 0.13 M *n*-butanol. However, when DOPC was the continuous phase, T_m hysteresis was observed above 0.2 M *n*-butanol.

Evidence for interdigitation from T_p and T_m is contradictory and was addressed by considering the melting enthalpies (Figure 3). ΔH_m was directly proportional to the DPPC concentration, which shows that the DPPC present within the membranes existed within gel phases and melted. Increases in ΔH_m were observed with increasing *n*-butanol concentration in all DPPC/DOPC membranes, and upon cooling, ΔH_m was higher than that for heating. ΔH_m hysteresis became most pronounced at or above 0.13 M *n*-butanol at all DPPC:DOPC ratios. While trends in T_p and T_m were contradictory, trends in T_m and ΔH_m indicate that DPPC was interdigitated at 0.13 M

dx.doi.org/10.1021/jp301340k | J. Phys. Chem. B 2012, 116, 5919−5924

n-butanol up to equimolar DPPC:DOPC ratios and at 0.2 M when DOPC was the continuous phase.

***n*-Butanol Partitioning (K_p).** Calculated *n*-butanol partitioning coefficients (K_p) were 62, 54, and 45 at DPPC:DOPC ratios of 1:0, 3:1, and 1:1. These are based on ΔT_m (eq 2) and reflect the amount of *n*-butanol in the DPPC phases during melting. The results suggest that increasing DOPC concentration led to a decrease in *n*-butanol partitioning into DPPC. K_p was also measured at 25 °C as a function of *n*-butanol and DOPC concentration (Figure 4A). Corresponding values for the number of *n*-butanol molecules per lipid are shown (Figure 4B). For DPPC, K_p was dependent on the phase state: 101 in the $L_{\beta'}$ phase (0.03 M *n*-butanol) and 200 in the $L_{\beta I}$ phase (0.27 M *n*-butanol). Greater partitioning into $L_{\beta I}$ phases was consistent with previous results.[12] It should be noted that the K_p values were larger than previously reported for gel or interdigitated DPPC.[12]

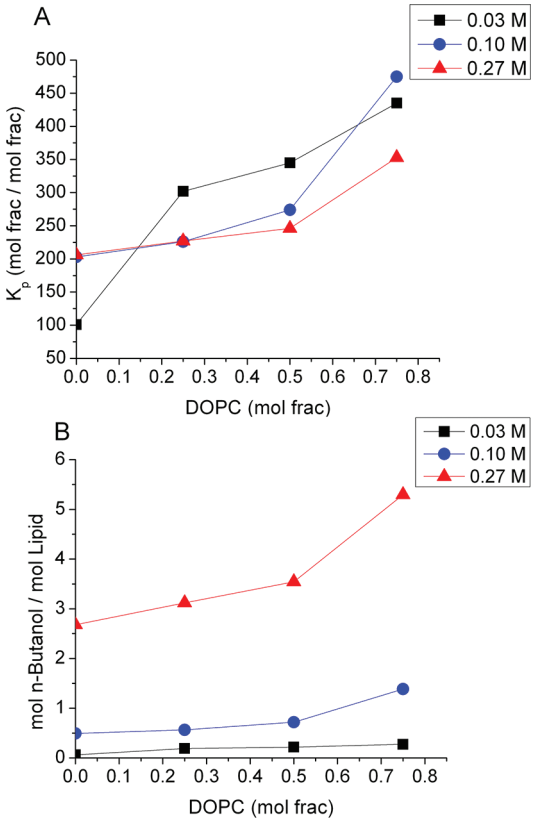

Figure 4. (A) Aqueous/membrane *n*-butanol partition coefficients for DPPC/DOPC liposomes as a function of DOPC fraction and *n*-butanol concentration. Measurements were performed at 25 °C. (B) Number of *n*-butanol molecules per lipid determined from K_p.

For DPPC/DOPC, the membranes were in coexisting $L_{\beta'}$ (DPPC) + L_α (DOPC) phases at 0.03 M and coexisting $L_{\beta I}$ (DPPC) + L_α (DOPC) phases at 0.10 and 0.27 M. *n*-Butanol partitioning increased proportional to the DOPC content when the membrane was in a $L_{\beta'}$ + L_α state. In contrast, the increase in K_p was modest when the membrane was in a $L_{\beta I}$ + L_α state. Only at a DPPC:DOPC ratio of 1:3, when DOPC was the continuous phase, did K_p increase. Comparing measured and calculated K_p values suggests that, below the interdigitation concentration, additional *n*-butanol partitioning was dependent on DOPC concentration and that the presence of DOPC did not increase partitioning into DPPC. However, above the interdigitation concentration K_p was dependent upon which lipid was the continuous phase.

Membrane Fluidization. Fluorescence anisotropy was conducted using the probe DPH to assess membrane fluidization due to lipid disordering. Anisotropy, $\langle r \rangle$, is shown in Figure 5 at 25 and 50 °C as a function of the *n*-butanol concentration. Increases in $\langle r \rangle$ denote lipid ordering or a decrease in membrane fluidity while decreases in $\langle r \rangle$ denote lipid disordering or an increase in membrane fluidity. At 25 °C, increasing the *n*-butanol concentration had little effect on $\langle r \rangle$ in DPPC, which was between 0.29 and 0.32 with heating or cooling (Figure 5). This indicates that the lipid ordering experienced by DPH was similar in gel and interdigitated gel phases. At 50 °C there was modest fluidization that shows increasing *n*-butanol concentration led to lipid disordering in the fluid phase.

At DPPC:DOPC ratios of 3:1 and 1:1, DPH anisotropy at 25 and 50 °C was similar to that for DPPC at low *n*-butanol concentrations. This shows that DPH preferentially partitioned into the $L_{\beta'}$ or L_α DPPC phase. However, above a critical *n*-butanol concentration (0.23 and 0.14 M, respectively) a sharp decrease in $\langle r \rangle$ was observed at both temperatures. When DOPC was the continuous phase, greater membrane fluidity was observed over the entire range of *n*-butanol concentrations when compared to the other membranes. There was also a pronounced $\langle r \rangle$ hysteresis with heating and cooling that indicates reorganization within the membrane.

DISCUSSION

For DPPC, it has been reported that *n*-butanol partitioning is greater in L_α phases than in $L_{\beta'}$ phases.[12] Although the same information is not available for membranes with saturated verses unsaturated lipids, previous work for ethanol has shown that partitioning into unsaturated L_α membranes is ~4-fold greater than into saturated L_α membranes.[10] While homogeneous membranes have been well studied, there is no direct information available on the partitioning behavior in mixed saturated/unsaturated membranes (for ethanol or *n*-butanol) or on how the partitioning affects membrane structure.

Heterogeneous membranes, specifically those containing DPPC and DOPC, attract interest due to their unique phase behavior and relevance as model membranes. However, conflicting results have been published for gel-fluid phase coexistence in DPPC/DOPC membranes. Microscopy studies on giant unilamellar vesicles (GUVs) have shown that when DPPC is in abundance, $L_{\beta'}$ and $P_{\beta'}$ phases coexist with DOPC (L_α) .[23] Up to 50% DOPC, gel DPPC was the continuous phase and contained fluid DOPC domains, while above 50% DOPC, DOPC was continuous and contained DPPC domains. For DOPC concentrations of 50% and greater, only the $P_{\beta'}$ was observed. Wide-angle X-ray spectroscopy studies on multilamellar vesicles (MLVs) contradict these results and indicate that, at equimolar DPPC:DOPC, the gel DPPC phase does not form a $L_{\beta'}$ phase, but rather an untilted $L_{\beta'}$-like phase.[24] Our DSC results show that a pretransition did occur at all DPPC:DOPC ratios in the absence of *n*-butanol, but quickly disappeared with increasing DOPC and *n*-butanol concentration. We do not attribute the disappearance of the pretransition to interdigitation, but rather a cooperative effect of DOPC + *n*-butanol that restricts lipid tilt and eliminates the $L_{\beta'} \rightarrow P_{\beta'}$ transition. This is based in part on evidence of T_m and ΔH_m hysteresis that infers a common interdigitation concen-

dx.doi.org/10.1021/jp301340k | J. Phys. Chem. B 2012, 116, 5919−5924

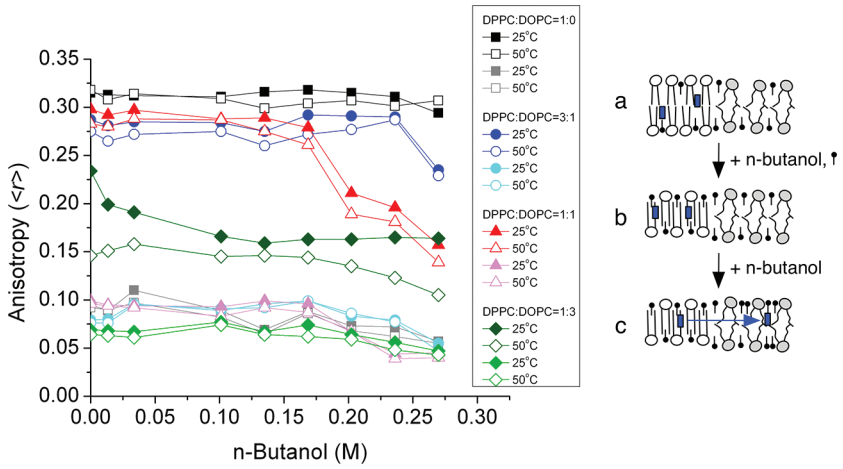

Figure 5. DPH fluorescence anisotropy at DPPC:DOPC ratios of (square) 1:0, (triangle) 3:1, (circle) 1:1, and (diamond) 1:3 as a function of *n*-butanol concentration at 25 °C (■, blue ●, red ▲, green ◆) and 50 °C (gray ■, light blue ●, magenta ▲, light green ◆). Filled symbols represent heating scans and unfilled symbols represent cooling scans. (right) Schematic depicting the location of DPH within the membranes. DPH preferentially resides in the DPPC phase (a, b) until a critical *n*-butanol concentration is reached. DPH then partitions into the DOPC phase (c).

tration between 0.1 and 0.13 M *n*-butanol when gel DPPC is the continuous phase.

Surface tension (γ) in lipid membranes is related to the area compressibility modulus ($\gamma \propto K_A$) and, with solute concentration (c), the partition coefficient ($d\Delta\gamma/dc \equiv K_p$). K_A is lower for fluid phases and unsaturated lipids than for gel phases and saturated lipids. Hence, increasing DOPC and/or *n*-butanol concentrations would lower membrane surface tension and reduce T_m. This was not observed in the absence of *n*-butanol, consistent with the observation that DPPC (continuous or as domains) was not influenced by DOPC at the conditions examined. However, a reduction in T_m was observed in the presence of *n*-butanol below the interdigitation concentration. In this case, increasing the DOPC concentration up to an equimolar DPPC:DOPC ratio did not affect this T_m reduction. This suggests that increasing DOPC concentration did not increase *n*-butanol partitioning into gel DPPC and that increases in K_p, when gel DPPC was the continuous phase, can be attributed to additional partitioning into fluid DOPC. This is in agreement with K_p calculated from DSC.

K_p increased linearly with DOPC concentration below the *n*-butanol interdigitation concentration and appeared to be independent of which phase was continuous. The linear relationship suggests that greater partitioning correlated with greater fluid phase fraction. Above the interdigitation concentration, K_p was dependent upon which phase was continuous. Up to a DPPC:DOPC ratio of 1:1, interdigitated DPPC was the continuous phase and there was a modest increase in K_p. This indicates that *n*-butanol had a similar affinity for the interdigitated and fluid phases, which has been shown for ethanol.[20] At a DPPC:DOPC ratio of 1:3, fluid DOPC was the continuous phase, and there was a notable increase in K_p. At this stage we attribute the increase in K_p to *n*-butanol partitioning at the $L_{\beta I}/L_\alpha$ interface. This concept is supported by theoretical[25] and experimental[25−27] evidence that the dynamic wetting layer at gel/fluid interfaces become more influential when the fluid phase fraction is increased and becomes the continuous phase.

Fluorescence anisotropy provides additional insight into membrane structure. Assuming that DPH has equal affinity for gel and fluid phases,[28] $\langle r \rangle$ would represent the weighted average of DPPC gel and DOPC fluid domains. The anisotropy of DPPC at 25 °C was greater than 0.3 across the range of *n*-butanol concentrations, which shows that the lipid ordering experienced by DPH in the $L_{\beta I}$ and $L_{\beta'}$ phases was similar. For DOPC at 25 °C without *n*-butanol, $\langle r \rangle$ was 0.1 (not shown). The weighted average of $\langle r \rangle$ calculated at DPPC:DOPC ratios of 3:1, 1:1, and 1:3 are approximately 0.25, 0.2, and 0.15, respectively. This was not observed at ratios of 3:1 or 1:1 until *n*-butanol concentrations of 0.27 and 0.2 M were reached, respectively. Below these concentrations, $\langle r \rangle$ was consistent with gel DPPC phases ($L_{\beta'}$ or $L_{\beta I}$). DPH aligns parallel to lipid tails near the bilayer center, and its apparent preference for DPPC rather than DOPC may reflect unfavorable tail packing within DOPC that leads to large areas per headgroup (more interfacial void space) and exposes the hydrophobic core to water. When *n*-butanol is added, it partitions to the lipid/water interface and occupies these void spaces. This shields the hydrophobic core from water and makes it more favorable for DPH to partition into DOPC. This concept is supported by the high number of *n*-butanol molecules per lipid at high DOPC concentrations (Figure 4B). Considering that this occurs above the interdigitation concentration, we can conclude that DPPC, when it was the continuous phase, was interdigitated before DPH partitioned into DOPC. When DOPC was the continuous phase, $\langle r \rangle$ appeared to reflect the weighted average.

The cooperative effects of DOPC + *n*-butanol proceeded as followed based on our interpretation of the data (Figure 6). Below the interdigitation concentration, *n*-butanol partitioning increased with DOPC concentration proportional to the fluid phase fraction. This resulted in DPPC converting from a $L_{\beta'}$ phase to an untilted L_β-like phase, upon which point the $P_{\beta'}$ phase was not observed. Above the interdigitation concentration, *n*-butanol had similar affinity for $L_{\beta I}$ and L_α phases, and there was little change in the partition coefficient when DPPC was the continuous phase. However, when DOPC was the continuous phase, *n*-butanol partitioning increased due to the dynamic wetting effect at the gel/fluid interface.

■ CONCLUSIONS

Results from this work depict a cooperative effect of DOPC + *n*-butanol on membrane phase behavior that was dependent on *n*-butanol concentration and which phase (DPPC or DOPC)

dx.doi.org/10.1021/jp301340k | J. Phys. Chem. B 2012, 116, 5919−5924

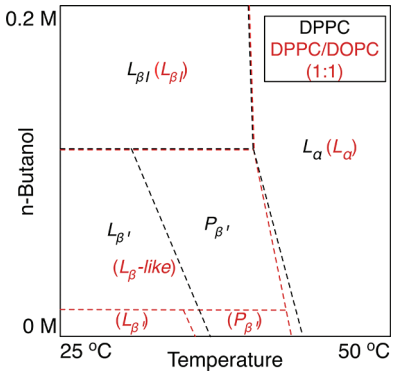

Figure 6. Schematic depicting the phase behavior of DPPC (black) and DPPC/DOPC (1:1; red, phases further indicated in parentheses) as a function of *n*-butanol concentration and temperature.

was continuous. Below the interdigitation concentration with a continuous gel DPPC phase, the total *n*-butanol partitioning increased proportional to the fluid phase fraction (DOPC), but partitioning into DPPC was unchanged. In this case DOPC alone did not eliminate ripple gel formation by DPPC, but DOPC + *n*-butanol did by promoting a L_β-like DPPC phase. Fluidization results showed that the fluorophore preferentially partitioned into gel or interdigitated gel phases at low *n*-butanol concentrations but distributed more evenly between DPPC and DOPC at high *n*-butanol concentrations (twice that for interdigitation). We propose that this was achieved by *n*-butanol filling the membrane/water interface and reducing unfavorable tail packing conditions normally experienced DOPC that expose the hydrophobic region to water. This study infers a cooperative effect of unsaturated lipids and alcohols in heterogeneous membranes, which aids our understanding of how membranes with mixtures of saturated to unsaturated lipids restructure in response to alcohols.

AUTHOR INFORMATION

Corresponding Author

*E-mail bothun@egr.uri.edu; Tel +1-401-874-9518; Fax +1-401-874-4689.

Notes

The authors declare no competing financial interest.

ACKNOWLEDGMENTS

This work was supported by the National Science Foundation Energy for Sustainability program (CBET-0966818). We acknowledge Dr. Katherine Taconi for her support and insight and the contributions of Evan Mello, an undergraduate student funded through the National Science Foundation Rhode Island EPSCoR Summer Undergraduate Research Fellowship program.

REFERENCES

(1) Herold, L. L.; Rowe, E. S.; Khalifah, R. G. *Chem. Phys. Lipids* **1987**, *43*, 215.
(2) Ho, C. J.; Stubbs, C. D. *Biochemistry* **1997**, *36*, 10630.
(3) Krill, S. L.; Knutson, K.; Higuchi, W. I. *J. Controlled Release* **1993**, *25*, 31.
(4) Löbbecke, L.; Cevc, G. *Biochim. Biophys. Acta, Biomembr.* **1995**, *1237*, 59.
(5) Ly, H. *Biophys. J.* **2004**, *87*, 1013.
(6) Patra, M.; Salonen, E.; Emma, T.; llpo, V. *Biophys. J.* **2006**, *90*, 1121.
(7) Pillman, H. A.; Blanchard, G. J. *J. Phys. Chem. B* **2010**, *114*, 3840.
(8) Reeves, M. D.; Schawel, A. K.; Wang, W.; Dea, P. *Biophys. Chem.* **2007**, *128*, 13.
(9) Rowe, E. S.; Zhang, F.; Leung, T. W.; Parr, J. S.; Guy, P. T. *Biochemistry* **1998**, *37*, 2430.
(10) Terama, E.; Ollila, O. H. S.; Salonen, E.; Rowat, A. C.; Trandum, C.; Westh, P.; Patra, M.; Karttunen, M.; Vattulainen, I. *J. Phys. Chem. B* **2008**, *112*, 4131.
(11) Vierl, U.; Löbbecke, L.; Nagel, N.; Cevc, G. *Biophys. J.* **1994**, *67*, 1067.
(12) Zhang, F.; Rowe, E. S. *Biochemistry* **1992**, *31*, 2005.
(13) Bowles, L. K.; Ellefson, W. L. *Appl. Environ. Microbiol.* **1985**, *50*, 1165.
(14) Vollherbst-Schneck, K.; Sands, J. A.; Montenecourt, B. S. *Appl. Environ. Microbiol.* **1984**, *47*, 193.
(15) Cantor, R. S. *J. Phys. Chem. B* **2001**, *105*, 7550.
(16) Marques, J. T.; Viana, A. S.; De Almeida, R. F. M. *Biochim. Biophys. Acta, Biomembr.* **2011**, *1808*, 405.
(17) Bangham, A. D.; Standish, M. M.; Watkins, J. C. *J. Mol. Biol.* **1965**, *13*, 238.
(18) Lakowicz, J. R.; Prendergast, F. G.; Hogen, D. *Biochemistry* **1979**, *18*, 520.
(19) Parasassi, T.; Conti, F.; Glaser, M.; Gratton, E. *J. Biol. Chem.* **1984**, *259*, 14011.
(20) Kranenburg, M.; Vlaar, M.; Smit, B. *Biophys. J.* **2004**, *87*, 1596.
(21) Parasassi, T.; Stasio, G. D.; Rusch, R. M.; Gratton, E. *Biophys. J.* **1991**, *59*, 466.
(22) Miccoli, L.; Szczepaniak, C.; Dumas, D.; Savonniere, S.; Muller, S.; Carr, M. C.; Donner, M. *J. Fluoresc.* **1993**, *3*, 251.
(23) Li, L.; Cheng, J.-X. *Biochemistry* **2006**, *45*, 11819.
(24) Mills, T. T.; Huang, J.; Feigenson, G. W.; Nagle, J. F. *Gen. Physiol. Biophys.* **2009**, *28*, 126.
(25) Jorgensen, K.; Mouritsen, O. G. *Biophys. J.* **1995**, *69*, 942.
(26) Leidy, G.; Wolkers, W. F.; Jorgensen, K.; Mouritsen, O. G.; Crowe, J. H. *Biophys. J.* **2001**, *80*, 1819.
(27) Almeida, R. F. M. D.; Loura, L. M. S.; Fedorov, A.; Prieto, M. *Biophys. J.* **2002**, *82*, 823.
(28) Florinecasteel, K.; Feigenson, G. W. *Biochim. Biophys. Acta* **1988**, *941*, 102.